

Scalability of Hydrodynamic Simulations

Shikui Tang and Q. Daniel Wang

*Department of Astronomy, University of Massachusetts, Amherst, MA 01003;
tangsk@astro.umass.edu and wqd@astro.umass.edu*

ABSTRACT

Many hydrodynamic processes can be studied in a way that is scalable over a vastly relevant physical parameter space. We systematically examine this scalability, which has so far only briefly discussed in astrophysical literature. We show how the scalability is limited by various constraints imposed by physical processes and initial conditions. Using supernova remnants in different environments and evolutionary phases as application examples, we demonstrate the use of the scaling as a powerful tool to explore the interdependence among relevant parameters, based on a minimum set of simulations. In particular, we devise a scaling scheme that can be used to adaptively generate numerous seed remnants and plant them into 3D hydrodynamic simulations of the supernova-dominated interstellar medium.

Subject headings: methods: miscellaneous — galaxies: ISM — ISM: structure — supernova remnants

1. Introduction

Similar natural phenomena, which may occur on vastly different space and time scales, can often be treated in the same way. One well-known example is the similarity between a supernova (SN) in the interstellar medium (ISM) and a nuclear explosion in the earth atmosphere despite of their vastly different energies ($\sim 10^{51}$ ergs vs. $\sim 10^{21}$ ergs). Their blastwave structure and evolution may be mathematically approximated by the same self-similar Sedov-Taylor solution (Sedov 1959), with an appropriate scaling according to the energy and ambient medium density. Such self-similarity, though often limited in its applicability (e.g., the evolution needs to be adiabatic; the mass of the ejecta is negligible; etc.), has been widely used in astrophysical studies.

The scalability of a hydrodynamic process, as will be demonstrated in the present paper, has a much broader application. Here we explore how the solution (or simulation) for one physical setup can be scaled to another, when the underlying governing equations are the same. The self-similarity is then only a special case of the scalability. Therefore, the scalability analysis provides a systematic way to examine the physical parameter space, based on a limited number of solutions. As a specific example, we apply our scalability analysis to the study of the SN remnant (SNR) evolution in various environments and at different evolutionary stages.

The scalability has the same idea as the *homology relations*, which are used in studying the interior structure of stars in complete equilibrium (both hydrostatic and thermal; e.g., Kippenhahn & Weigert 1994). A unique scaling relation to study the SNR evolution was probably first introduced by Sgro (1972). Chevalier (1974) discussed the same scaling relation to analyze the evolution of SNRs of different setups with a limited number of simulations. By recognizing that one simulation of a particular SNR can be used to describe a family of SNRs if they all have the same $E_{sn}n_0^2$ (where n_0 is the number density of ambient medium and E_{sn} is the SN energy, see §2.2 for further discussion), Shelton et al. (1999) pointed out the usefulness of the scaling in interpreting observations with a few simulations. These discussions, though limited in their scope, have demonstrated the potential of using the scalability in the study of SNRs.

In the present paper, we attempt to give a systematic examination of the scalability of SNR solutions and simulations and provide specific application examples. The initial motivation of this work is to find an effective method to generate 1D SNR seeds that can be embedded into 3D hydrodynamic simulations of the SN-dominated ISM, particularly in galactic bulges where the ISM is dominated by diffuse hot gas. The SNR evolution in such ambient medium in general cannot be described by the self-similar Sedov-Taylor solution, which assumes a cool ambient medium (hence with no energy content). In fact the evolution depends on both the density and temperature of the ambient medium (Tang & Wang 2005). Each 3D simulation needs, for example, more than 10^4 SNR seeds for a bulge of an even moderate stellar mass $\sim 10^{10} M_\odot$, as in our Galaxy or M31, over a few times their dynamic time scales ($\sim 10^8$ years). The seed embedding, worked with an adaptive mesh refinement scheme, can effectively extend such a 3D simulation to include the subgrid evolution of SNRs. Here the subgrid evolution means that the structure of SNR seeds results from the evolution on scales much smaller than the highest spatial resolution available in the 3D simulations. The size of an embedded SNR seed cannot be too big (in order to use the 1D simulation properly) or too small (to be within the limited dynamic range of a 3D simulation). Therefore, we should adaptively select suitable SNR seeds according to the local density and temperature (values and gradients) of the environments. For each selected SNR seed, we need the 1D radial density, temperature, and velocity profiles, with proper normalizations to guarantee the mass, momentum, and energy conservations of the embedding into the 3D simulation (Tang et al. 2009). In principle, we could draw the seeds (with some interpolations) from a library of the profiles in a grid of the three parameters: SNR radius as well as the density and temperature of the ambient gas (the explosion energy and ejecta mass are assumed to be the same for all SNe; otherwise a larger parameter space is required for such a library). Clearly, this approach of generating and using such a large library is not elegant, if practical. Instead, we find that we can use the scalability to generate the seeds based on a very limited number of 1D SNR simulations. We describe this simple approach as an application example.

In §2 we show how to deduce the scaling relation starting from the basic gas dynamics equations and what the constraints of the scaling are. In §3 we apply the scaling to specific cases of the SNR evolution. In particular, we demonstrate how we use the scaling to generate SNR seeds for the

3D simulations with a few 1D simulations and how to correctly interpret the simulated relations. Finally in §4, we discuss the potential use of the scaling in a broader context.

2. Scaling Scheme

2.1. Basic Idea

For a system passively evolving without source terms, the dynamics can be described by the following equations:

$$\frac{\partial \rho}{\partial t} + \nabla \cdot (\rho \mathbf{v}) = 0, \quad (1)$$

$$\frac{\partial \rho \mathbf{v}}{\partial t} + \nabla \cdot (\rho \mathbf{v} \mathbf{v}) + \nabla P = 0, \quad (2)$$

$$\frac{\partial \rho e}{\partial t} + \nabla \cdot [(\rho e + P) \mathbf{v}] = 0, \quad (3)$$

where ρ , \mathbf{v} , and P denote density, velocity vector, and pressure, while the total specific energy e can be expressed as $e = \frac{p}{(\gamma-1)\rho} + \frac{1}{2}\mathbf{v}^2$ for ideal gas. This set of equations is in a closed form; i.e., we can solve five independent unknown scalar variables (ρ , \mathbf{v} , and P ; t and the spatial position are explicitly known variables), from the five equations (because Eq. 2 can be decomposed in three scalar equations). If the thermal state of the gas is of interest, the equation of state is needed:

$$p = R_\mu \rho T \quad (4)$$

where R_μ is the equivalent ideal gas constant¹ and T is the gas temperature. The scaling scheme can be found by converting each variable² Q as $Q\lambda^{i_Q}$ (where λ can be any positive value) and solving them for i_Q (to recover the equations before the conversion). It can be found that the same solution holds if

$$i_\rho - i_t = i_\rho + i_v - i_L, \quad (5)$$

$$i_\rho + i_v - i_t = i_\rho + 2i_v - i_L = i_p - i_L, \quad (6)$$

$$i_\rho + i_e - i_t = i_\rho + i_e + i_v - i_L = i_p + i_v - i_L, \quad (7)$$

$$i_p = i_\rho + i_T, \quad (8)$$

¹Note that $R_\mu = k/\mu m_p$, where k is the Boltzmann constant, m_p is the proton mass, and μ is the average atomic weight. The value of μ depends on the gas ionization state and might change with temperature. For hot gas μ only weakly depends on temperature so R_μ can be approximated as a constant. And as long as the scaling is within a limited temperature range, the small variation in μ can be neglected.

²These variables include fundamental quantities such as length (L), time (t), and mass (M) and other physical quantities such as density (ρ), pressure (p), velocity (v), specific energy (e), total energy (E), etc.

which can be simplified as

$$i_v = i_L - i_t, \quad (9)$$

$$i_\rho = i_p - 2i_L + 2i_t, \quad (10)$$

$$i_e = 2i_L - 2i_t, \quad (11)$$

$$i_T = 2i_L - 2i_t. \quad (12)$$

Therefore, only three indices are independent in Eqs. (9)–(12). If we consider i_L , i_t , and i_M to be independent, other indices can then be expressed as

$$i_v = i_L - i_t, \quad (13)$$

$$i_e = 2i_L - 2i_t, \quad (14)$$

$$i_\rho = i_M - 3i_L, \quad (15)$$

$$i_p = i_M - i_L - 2i_t, \quad (16)$$

$$i_E = i_M + 2i_L - 2i_t, \quad (17)$$

$$i_T = 2i_L - 2i_t. \quad (18)$$

Eqs. (13)–(17) show that the scaling relation of the physical quantities can be directly inferred from their dimensions based on the basic units of mass, length, and time. Indeed there is no constraint on the choice of i_L , i_t , or i_M from the governing equations (1)–(3) for this simple case (see also Ryutov et al. 1999 where such a property of the equations is called Euler similarity). But i_T is restricted by i_L and i_t through the equation of state. This constraint is given because R_μ is fixed (to a number with non-vanishing dimension hard-wired in a specific simulation), which reduces one degree of freedom for the scaling of the pressure, density, and temperature. In other words, although we have four basic units for the ideal gas hydrodynamics (i.e., mass, length, time, and temperature), we are only able to freely change three of them when scaling from one case to another, i.e., i_M and two other indices from the pool of i_L , i_t , and i_T .

A special class of the scalability is the self-similar solution. In this case, clearly only one solution is needed. However, such a solution, if exists, may not be easily expressed in an analytic form and may be applicable only asymptotically (e.g., when the effect of the initial condition becomes negligible). In general, one may resort to a simulation to reach the solution. Thus it can be studied as part of the scalability problem considered here.

2.2. Additional Constraints

If Eqs. (1)–(3) have source terms, more constraints may then be placed on the scaling relation. For example, the inclusion of the thermal conduction term, $q = \nabla \cdot [\kappa(T)\nabla T]$, at the r.h.s in equation (3) requires

$$i_M - 3i_t + i_L - 3.5i_T = 0 \quad (19)$$

for non-saturated thermal conduction in which $\kappa(T) = k_0 T^{5/2}$, where $k_0 \sim 9 \times 10^{-7} \text{ erg cm}^{-1} \text{ s}^{-1} \text{ K}^{-7/2}$ is the Spitzer conduction coefficient (Spitzer 1962). For saturated thermal conduction ($q \propto \rho c_s^3$) no constraint like Eq. (19) is required because it does not require an extra coefficient with a non-vanishing dimension. The constraint from a radiative cooling term $-n_H n_e \Lambda(T)$ in the same equation depends on the form of emissivity $\Lambda(T)$. For optically thin primordial gas of temperature larger than $5 \times 10^6 \text{ K}$, for example, the emissivity can be approximated as $\Lambda(T) = \Lambda_0 T^{1/2}$ where $\Lambda_0 \sim 10^{-27} \text{ erg cm}^6 \text{ s}^{-1} \text{ K}^{-1/2}$ and the constraint becomes

$$i_M + 3i_t - 5i_L + 0.5i_T = 0. \quad (20)$$

In general the cooling rate $\Lambda(T)$ does not have such a simple power law form, so the scaling relation is

$$i_T = 0; \quad i_L = i_t; \quad i_M = 2i_t \quad (21)$$

when combined with Eq. (18), which gives the unique scaling relation adopted by Sgro (1972). This scaling relation also makes $E_{sn} n_0^2$ an invariant (i.e., $i_E + 2i_\rho = 0$) as used in Shelton et al. (1999).

Additional physical constraints other than those from the governing equations may need to be placed on the scalability. For example, the scaling requires $i_E=0$ and/or $i_\rho=0$ between solutions with an identical explosion energy and/or ambient density. Note that we have three degrees of freedom for all the power indices, if the number of the constraints is less than three (i.e., at least one index is free to change), the solution is then scalable; otherwise the solution pertains only to a particular problem.

Implicit constraints on the scaling relation may be imposed by initial conditions as well. Specifically, when we scale one solution $[\rho_a(r_a, t_a), T_a(r_a, t_a), \dots]$ to another $[\rho_b(r_b, t_b), T_b(r_b, t_b), \dots]$, the corresponding initial condition needs to be scaled in the same way. For example, a particular scaling relation can be determined by specifying i_M , i_L , and i_t , which in turn determines i_v , i_ρ and other indices via Eqs. (13)–(18). This scaling relation demands that the corresponding initial conditions should be related by

$$\rho_b(r_b, t_{b0}) = \rho_a(r_a, t_{a0}) \lambda^{i_\rho}, \quad (22)$$

$$v_b(r_b, t_{b0}) = v_a(r_a, t_{a0}) \lambda^{i_v}, \quad (23)$$

and other quantities for

$$r_b = r_a \lambda^{i_L}, \quad t_{b0} = t_{a0} \lambda^{i_t}. \quad (24)$$

It is such demands on the initial condition that often make one problem be unique from others (limiting the scalability of their solutions), even if all have the same governing equations and characteristic quantities such as total energy and mass (see §3.5 for further discussion). In the following we assume that the scalable solutions do have the required initial conditions unless being explicitly expressed otherwise.

3. Application Examples

We use the evolution of SNRs as a simple example to demonstrate how the above described scalability can be used. The scalability of an SNR solution or simulation depends on its evolutionary stage and on the properties of the ambient medium.

3.1. Sedov-Taylor Solution

If the ejecta mass can be neglected and the ambient gas temperature can be approximated to be zero, then the evolution of the SNR can be described by the Sedov-Taylor solution, which depends only on the explosion energy E_{sn} and the ambient gas density ρ_0 . The solution can be obtained either numerically (Taylor 1950) or analytically (Sedov 1959). In particular the self-similar solution of the shock front,

$$r_{sh}(t) = \xi \left(\frac{E_{sn} t^2}{\rho_0} \right)^{1/5}, \quad (25)$$

is widely used, where $\xi \simeq 1.15$ for ideal gas with the specific heat ratio $\gamma=5/3$. From the scaling point view, following Eq. (15) and (17), we have $5i_L = i_E + 2i_t - i_\rho$ (i.e., $r \propto E^{1/5} t^{2/5} \rho^{-1/5}$), which just the same relation shown in Eq. (25). Furthermore, for the same remnant, we have $i_E=0$ and $i_\rho=0$, hence $i_L=0.4i_t$, $i_v=-0.6i_t$, $i_p=-1.2i_t$, and other indices following Eqs. (13)–(18). It shows that for a self-similar solution all the non-zero indices are proportional to i_t . This allows the scaling from one solution at any particular time to another.

Of course, the Sedov-Taylor solution applies only when the SN ejecta and ambient temperature can be neglected. Otherwise, this self-similar solution cannot be applied. But the scaling may still be useful.

3.2. SNRs in Hot Gas

If the ambient temperature is not negligible, a generalized formula for the SNR shock front can be expressed as (Tang & Wang 2005)

$$r_{sh}(t) = \int_0^t c_s \left(\frac{t_c}{t} + 1 \right)^{3/5} dt, \quad (26)$$

$$= \xi \left(\frac{E_{sn} t^2}{\rho_0} \right)^{1/5} F \left(-\frac{3}{5}, \frac{2}{5}, \frac{7}{5}; -\frac{t}{t_c} \right), \quad (27)$$

where c_s is the sound speed of the ambient medium, F is the generalized hyper-geometric function and is equal to 1.16 when $t = t_c$ which is defined as

$$t_c = \left[\left(\frac{2}{5} \xi \right)^5 \frac{E_{sn}}{\rho_0 c_s^5} \right]^{1/3}. \quad (28)$$

This modification accounts for the energy content of the swept-up ambient medium. Note that Eq. (27) is very similar to the Sedov-Taylor solution Eq. (25) except for the modification term F . When $t > t_c$, the shock front evolution significantly deviates from the Sedov-Taylor solution. If the temperature of the ambient medium is zero, then $t_c \rightarrow \infty$, $F = 1$, and Eq. (27) is the same as Eq. (25). In general, the solution in this case is no longer self-similar. The reason is that the evolution requires $i_E=0$, $i_\rho=0$, and $i_p=0$. Thus all the indices are fixed to be zero. The internal profiles change with time and cannot be scaled from one time to another.

But the solution is still scalable between remnants evolving in different environment. As illustrated in the following, one simulation in a particular environment is sufficient to infer specific SNR solutions in other environments with different ambient density and/or temperature.

3.3. SNR Seed Generation for 3D Simulations

The scalability has a particularly important application in planting SNR seeds in 3D simulations of the ISM. Suppose that each SNR in such a 3D simulation has the same explosion energy (i.e., $i_E=0$)³. For convenience, we can choose the remaining two free indices to be the power indices of the density and temperature, which can be directly measured in the simulation. The scaling relation can then be simplified as

$$i_E = 0, \tag{29}$$

$$i_M = -i_T, \tag{30}$$

$$i_L = -i_T/3 - i_\rho/3, \tag{31}$$

$$i_t = -5i_T/6 - i_\rho/3, \tag{32}$$

$$i_v = 0.5i_T. \tag{33}$$

Therefore, we can build a library of SNR templates. Each consists of the radial profiles of density, temperature, and velocity when the shock front of the SNR has a certain radius or age. These templates can be obtained from a 1D simulation of an SNR evolving in a uniform ambient medium of density ρ_a and temperature T_a . Using the library and the above scaling relation, we can generate SNR seeds at any time and at any position of the 3D simulation. The time and position of each SN can be realized randomly according to the Poisson statistics and the stellar distribution of a galactic bulge, for example. The procedure to embed an SNR seed into the 3D simulation is as follows:

- 1) At the time step just after the SN and around its position, determine a spherical region of radius r_{max} , within which T and ρ are sufficiently uniform so that a 1D SNR seed is a reasonable

³In principle, the explosion energy can vary as well and the resultant scaling relation can be obtained in a similar way, and we do not need to expand the parameter space of the SNR library. Without losing generality, however, we have assumed the canonical value $E_{sn} = 10^{51}$ erg for Type Ia SNe.

- approximation (in practice, a fraction of the radius $r_b = \eta r_{max}$ may be used, where $\eta < 1$);
- 2) Calculate the average density $\bar{\rho}$ and (mass-weighted) temperature \bar{T} in that region, and then determine the i_T and i_ρ : $i_\rho = \log_\lambda(\bar{\rho}/\rho_a)$ and $i_T = \log_\lambda(\bar{T}/T_a)$, which then determines i_L (Eq. 31);
 - 3) Search in the library for an SNR template which has the shock front radius of $r_a \simeq r_b \lambda^{-i_L}$ and the corresponding SNR age t_a ;
 - 4) Wait to a future elapsing time t_b of the simulation, when $t_b \simeq t_a \lambda^{i_t}$ is just satisfied, and read from the library the template (which may be interpolated to account for the difference between t_b and $t_a \lambda^{i_t}$, though not necessary if the time step is sufficiently small, compared to the t_b);
 - 5) Scale each profile Q of the template according to $Q \lambda^{i_Q}$;
 - 6) Plant the scaled profiles into the 3D simulation by replacing the values within r_b of the SN position (see Tang et al. 2009 for more details).

As the result, we have an adaptively configured SNR seed in the 3D simulation. This seed has a dynamically self-consistent structure expected for the SNR evolving in the local ambient medium, which is particularly important for accurately tracing the SNR structures and SN ejecta (see §3.4). We can therefore incorporate the sub-grid evolution of the SNR into the large-scale 3D simulation, which optimizes the use of the computational time and enlarges the covered dynamical range (Tang et al. 2009). It is not clear how such realism of the SNR seed and the adaptiveness of its planting can be realized in other simple way (e.g., assuming a uniform thermal energy deposition or other arbitrary profiles).

3.4. SN Ejecta and Scalable Initial Condition

When an SNR is young, the mass of the SN ejecta can be considerable. Assuming that the mass is the same for the SNRs in the consideration, we have $i_M=0$ as well as $i_E=0$ and $i_\rho=0$, as in the previous case. The SNR evolution is not self-similar and asymptotically approaches the Sedov-Taylor solution only when the swept-up mass is much greater than the ejecta mass (M_{ej}) and the swept-up energy is still negligible. But, the solution may still be scalable from one SNR to another. From Eqs. (29)–(33), we also have $i_T=0$ and $i_L=i_t=-i_\rho/3$. This means that one SNR evolving within an ambient medium of density ρ_a and temperature T_a can be scaled to another SNR of the density $\rho_b = \rho_a \lambda^{-3i_L}$ but of the same temperature; these two SNRs have their ages linked by $t_b = t_a \lambda^{i_L}$ and have the same swept-up masses and energies.

The same scheme introduced in the previous section can also be used for embedding SNR seeds including the ejecta. But in this case the library of SNR templates needs to be expanded because the scaling is now only accurate for SNRs evolving under the same ambient temperature. We can tabulate a series of SNRs simulated for a temperature grid. An interpolation may be used to generate any needed seed for a particular ambient gas temperature. If the grid is sufficiently fine, then such interpolation may not even be needed. For example, a logarithmical grid interval of 0.02 (i.e., only 50 SNR simulations are needed to cover an order of magnitude temperature range)

would introduce an uncertainty of $< 2\%$ in the ejecta mass, if the template with the nearest grid temperature is used. Such a small variation of the ejecta mass has a negligible effect on the SNR inner structure.

As indicated in §2.2, the scalability of an SNR solution also requires that its initial condition (i.e., SN ejecta profiles) to be scalable with respect to the surrounding medium. We find that such an initial condition can be set up within the uncertainty of SN ejecta models. We adopt the density and velocity profiles of a post-deflagration stellar remnant of a Type Ia SN as proposed by Dwarkadas & Chevalier (1998):

$$\rho(r) = \rho_s e^{1-r/r_s}, \quad v(r) = v_s \frac{r}{r_s}, \quad (34)$$

where ρ_s and v_s are the corresponding values at the characteristic radius r_s . The ejecta extends to a radius r_i so that

$$\int_0^{r_i} 4\pi r^2 \rho(r) dr = M_{ej}, \quad (35)$$

$$\int_0^{r_i} 2\pi r^2 \rho(r) v(r)^2 dr = E_{SN}. \quad (36)$$

Outside r_i is the ambient gas with an assumed uniform density ρ_a . To make the initial condition scalable, we set two dimensionless parameters,

$$f_i = \rho(r_i)/\rho_a, \quad (37)$$

and

$$f_m = 4\pi \rho_a r_i^3 / M_{ej}, \quad (38)$$

to be the same for all SNRs in the consideration. The four Eqs. (35)–(38) thus determine the four parameters: r_s, r_i, ρ_s , and v_s . From these equations, it is also easy to show that

$$2x^3(e^{1/x} - 1) - 2x^2 - x = (3f_i f_m)^{-1}, \quad (39)$$

$$v_s = \left(\frac{E_{SN}}{1.5 f_m f_i M_{ej} \beta} \right)^{1/2}, \quad (40)$$

where $x \equiv r_s/r_i$ and $\beta = 24x^3(e^{1/x} - 1) - (24x^2 + 12x + 4 + x^{-1})$. Thus x and v_s depend only on the assumed constants, f_i and f_m . Similarly, the ratio, $\rho_s/\rho_a = f_i e^{1/x-1}$, is again the same for various ambient densities. Thus, we can get any desirable SNR from a pre-simulated template with the above scalable initial condition.

To make the initial free expansion a good approximation to be described by Eq. (34), we need to have f_m much less than one (e.g., 10^{-4} in our examinations; no significant difference is found if $f_m=10^{-6}$). The parameter f_i (adopted to be 10) determines the shape of the initial ejecta profile; a larger f_i (which would result in a larger r_s), for example, and would give a flatter ejecta profile (i.e., more ejecta mass is distributed near r_i). But different choices of f_i (between 1 and 100) produce negligible effects. The same method can also be used to produce other forms of scalable initial ejecta profiles, e.g., a power law $\rho(r) \propto r^{-n}$ (e.g., Truelove & McKee 1999), or even a uniform distribution.

3.5. SNR Reverse Shock

With the scalable initial condition for the SN ejecta, we can further study how the evolution of an SNR reverse shock depends on various physical parameters. We demonstrate this by studying the return time of the reverse shock (t_R , i.e., when it reaches the center). Specifically, we examine the relation between t_R and the SN ejecta mass M_{ej} . In general, this relation cannot be determined in a pure analytical form, but can be easily identified in simulations.

Ferreira & de Jager (2008) have examined the relation based on a series of simulations, in which the SN ejecta is initially distributed uniformly within a radius of 0.1 pc and has a radial velocity increasing linearly outward. They show $t_R \propto M_{ej}^{3/4}$, in contrast to $t_R \propto M_{ej}^{5/6}$ predicted by Truelove & McKee (1999) from a simple dimensional analysis. Ferreira & de Jager (2008) suspect that this deviation may be caused by the non-zero ambient temperature assumed for the SNRs in their simulations. However, we find that the deviation is most likely due to their choice of the initial ejecta distribution, which is not scalable. Their initial condition for their $t_R - M_{ej}$ examination requires $i_E=0$, $i_\rho=0$, and $i_R=0$ (due to the specific choice of the initial ejecta radius), hence $i_M=0$. Therefore, each of their simulations is specific to a particular choice of M_{ej} and is not scalable to different M_{ej} value.

Using the scalable initial condition introduced in Eqs. (34)–(36), the simulations become scalable. Given $i_E=0$ and $i_\rho=0$, it is easy to show $i_t = \frac{5}{6}i_M$ (i.e., $t_R \propto M^{5/6}$). Based on four testing simulations with different M_{ej} we identify their return times. The simulated relation of t_R versus M_{ej} is shown in Fig. 1. This result is exactly the same as the expected from the scaling relation. The relations of t_R versus E_{sn} and ρ_a can be obtained similarly. Finally, we have

$$t_R \simeq 10^4 \left(\frac{\rho_a}{m_p} \right)^{-1/3} \left(\frac{M_{ej}}{1.4 M_\odot} \right)^{5/6} \left(\frac{E_{sn}}{10^{51} \text{ ergs}} \right)^{1/2} \text{ year.} \quad (41)$$

where $m_p = 1.67 \times 10^{-26} \text{ g cm}^{-3}$. The same scaling relation was also obtained for the reverse shock to reach the mantle of a core-collapse supernova exploded in a uniform medium (Reynolds & Chevalier 1984).

4. Discussion

We have described how a hydrodynamic solution or simulation may be scalable and how the scalability may be used to find out the underlying dependence on various physical parameters. In particular, we have demonstrated how to apply the scaling method to adaptively generate SNR seeds in large-scale 3D simulations of the ISM. We have also discussed how an assumed initial condition may affect the scalability, and specifically how the initial ejecta mass and its distribution are related to the return time of the SNR reverse shock.

Potentially, the scalability can be applied to a broad range of topics. In the applications that we have discussed, the ambient medium is assumed to be uniform on the relevant scales. But the

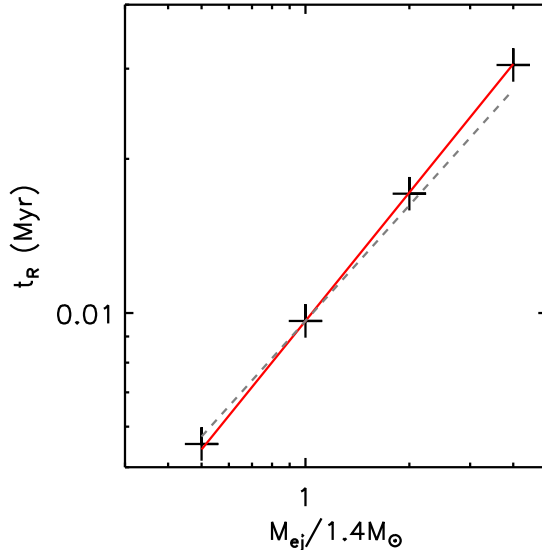


Fig. 1.— The relation between the reverse shock return time t_R and the ejecta mass M_{ej} for $M_{ej} = 0.7, 1.4, 2.8,$ and $5.6 M_{\odot}$. The solid line denotes the expected relation $t_R \propto M^{5/6}$, while the dotted line the relation $t_R \propto M^{-3/4}$ from Ferreira & de Jager (2008).

scaling method is still valid for any ambient medium with scalable profiles such as a power law density profile (e.g., $\rho \propto r^{-2}$ generated previously by a stellar wind). The medium may also be clumpy. As long as the inhomogeneity does not significantly affect the overall dynamics, which is normally true in the early stage of SNR evolution, the scaling method may still be applicable.

We have focused on SNRs in the hot tenuous medium for simplicity and for the need of our practical research projects on galactic bugles. But such SNRs are not limited to those from Type Ia SNe. Most of SNRs from core-collapsed SNe may also evolve in hot gas within superbubbles, because massive stars are born mostly in OB associations. This kind of SNRs are typically difficult to detect (e.g., Jiang et al. 2007), except for situations in which radiation from pulsar wind nebulae dominates (e.g., Crab Nebula and SNR G54.1+0.3; Lu et al. 2002). Luminous SNRs that are dominated by shock-heated hot gas typically originate from run-away stars and happen to be in a relatively dense ambient medium. Such SNRs probably represent a minority of the entire SNR population. In the late evolution of such an SNR, the cooling becomes important. Even in this case, the scaling method may still be useful (§ 2.2; Sgro 1972; Chevalier 1974; Shelton et al. 1999).

One may also find useful applications of the scheme that we have developed to adaptively generate SNR seeds and to embed them into large-scale 3D simulations of the ISM. In particular, existing simulations of the structure formation in the universe typically use various recipes to model the subgrid astrophysical processes. Such recipes are often hardly calibrated with any observations and/or are implemented in over-simplistic ways, constrained by the limited dynamic ranges avail-

able in these simulations. We believe that this problem may be circumvented by the application of a scheme similar to ours, which allows for a more realistic modeling of the subgrid evolution of important processes (e.g., individual SNRs, superbubbles around massive stellar clusters, superwind bubbles around galaxies, and feedback from active galactic nuclei into the intragroup/cluster medium). Bridging such subgrid evolution to the global hydrodynamics of the structure formation is badly needed to bring the simulations closer to the reality.

We thank Bill Mathews, R. A. Chevalier, and R. Shelton for useful comments on an early draft of this paper. The work is supported by NASA grants NNX06AI18G and TM7-8005X (via SAO/CXC).

REFERENCES

- Chevalier R. A. 1974, *ApJ*, 188, 501
- Dwarkadas V. V., & Chevalier R. A. 1998, *ApJ*, 497, 807
- Ferreira S. E. S., & de Jager O. C., 2008, *A&A*, 478, 17
- Jiang B., Chen Y., Wang Q. D., 2007, *ApJ*, 670, 1142
- Kippenhahn R., Weigert A. 1994, *Stellar structure and Evolution*, corrected 3rd printing, Springer-Verlag
- Lu F. J., Wang Q. D., Aschenbach B., Durouchoux P., Song L. M., 2002, *ApJ*, 568, L49
- Reynolds S. P., & Chevalier R. A., 1984, *ApJ*, 278, 630
- Ryutov D., Drake R. P., Kane J., Liang E., Remington B. A., Wood-Vasey W. M., 1999, *ApJ*, 518, 821
- Sgro A. 1972, Ph.D. thesis, Columbia Univ.
- Shelton R. L., Cox D. P., Maciejewski W., Smith R. K., Plewa T., Pawl A., & Rozyczka M. 1999, *ApJ*, 524, 192
- Sedov L. I 1959, *Similarity and Dimensional Methods in Mechanics*, translation from 4th Russian edition, Academic press New York and London
- Spitzer L., Jr. 1962, *Physics of Fully Ionized Gases* (2nd ed.; New Yor: Interscience)
- Tang S.,& Wang Q. D. 2005, *ApJ*, 628, 205
- Tang S., Wang Q. D., Mac Low M.-M., Joung M. R. 2009, *astroph/arXiv0902.0386*
- Truelove J. K., & McKee C. F., 1999, *ApJS*, 120, 299